Image registration accuracy of an in-house developed patient transport system for PET/CT+MR and SPECT+CT imaging

Samarin, Andrei ; Kuhn, Felix P ; Brandsberg, Fredrik ; von Schulthess, Gustav ; Burger, Irene A

Abstract: OBJECTIVE The aim of this study was to investigate the registration accuracy of a newly developed patient shuttle system that can integrate different scanners by patient transfer without repositioning for 'hardware'-based image fusion. We aimed to assess the registration accuracy of image fusion in two different settings: a trimodality PET/CT+MR system and a SPECT+CT system. MATERIALS AND METHODS In this prospective study, 43 patients underwent either sequential PET/CT and MR (n=31) or sequential SPECT and diagnostic CT (D-CT) (n=12). A side-loading patient shuttle system was used for patient transport. For PET/CT+MR, hardware-only coregistration was performed and then validated with anatomical landmarks on CT and MR. SPECT+D-CT image fusion was performed with external cobalt-57 markers and manual fusion. Registration accuracy was analysed by anatomical landmarks on the attenuation correction CT and the D-CT. RESULTS For the PET/CT+MR system, the mean offset between original CT and MR images in all 31 patients was 8.1±5.7 mm in the X-axis, 5±4 mm in the Y-axis and 4.9±5.6 mm in the Z-axis. The validation of the cobalt-57 marker-assisted SPECT+D-CT fusion yielded offsets of 0.7±1.7 mm in the X-axis, 2.1±1.7 mm in the Y-axis and 0.8±1.8 mm in the Z-axis. CONCLUSION Sequential PET/CT+MR and SPECT+D-CT imaging using a dedicated patient shuttle system is feasible, resulting in mean offsets between data sets of 10.7 mm using the gantry laser system and 2.4 mm with fiducial markers.

DOI: https://doi.org/10.1097/MNM.0000000000000229

Originally published at:
Samarin, Andrei; Kuhn, Felix P; Brandsberg, Fredrik; von Schulthess, Gustav; Burger, Irene A (2015). Image registration accuracy of an in-house developed patient transport system for PET/CT+MR and SPECT+CT imaging. Nuclear medicine communications, 36(2):194-200.
DOI: https://doi.org/10.1097/MNM.0000000000000229

Original article

Nuclear Medicine Communications

Image registration accuracy of an in-house developed patient transport system for PET/CT + MR and SPECT + CT imaging

Andrei Samarin[a], Felix P. Kuhn[a], Fredrik Brandsberg[b], Gustav von Schulthess[a] and Irene A. Burger[a]

Objective **The aim of this study was to investigate the registration accuracy of a newly developed patient shuttle system that can integrate different scanners by patient transfer without repositioning for 'hardware'-based image fusion. We aimed to assess the registration accuracy of image fusion in two different settings: a trimodality PET/CT + MR system and a SPECT + CT system.**

Materials and methods **In this prospective study, 43 patients underwent either sequential PET/CT and MR ($n = 31$) or sequential SPECT and diagnostic CT (D-CT) ($n = 12$). A side-loading patient shuttle system was used for patient transport. For PET/CT + MR, hardware-only coregistration was performed and then validated with anatomical landmarks on CT and MR. SPECT + D-CT image fusion was performed with external cobalt-57 markers and manual fusion. Registration accuracy was analysed by anatomical landmarks on the attenuation correction CT and the D-CT.**

Results **For the PET/CT + MR system, the mean offset between original CT and MR images in all 31 patients was 8.1 ± 5.7 mm in the *X*-axis, 5 ± 4 mm in the *Y*-axis and 4.9 ± 5.6 mm in the *Z*-axis. The validation of the cobalt-57 marker-assisted SPECT + D-CT fusion yielded offsets of 0.7 ± 1.7 mm in the *X*-axis, 2.1 ± 1.7 mm in the *Y*-axis and 0.8 ± 1.8 mm in the *Z*-axis.**

Conclusion **Sequential PET/CT + MR and SPECT + D-CT imaging using a dedicated patient shuttle system is feasible, resulting in mean offsets between data sets of 10.7 mm using the gantry laser system and 2.4 mm with fiducial markers.** ***Nucl Med Commun*** **00:000–000 © 2014 Wolters Kluwer Health | Lippincott Williams & Wilkins.**

Nuclear Medicine Communications 2014, **00**:000–000

Keywords: coregistration, image fusion, patient transporter, PET/CT + MR, sequential hybrid imaging, SPECT + CT

[a]Department of Nuclear Medicine, University Hospital of Zurich, Zurich and [b]Innovation Design Center, Thalwil, Switzerland

Correspondence to Andrei Samarin, MD, Department of Nuclear Medicine, University Hospital of Zurich, Ramistrasse 100, 8091 Zurich, Switzerland
Tel: +41 44 255 3555; fax: +41 44 255 4414; e-mail: andsam@gmail.com

Received 20 March 2014 **Revised** 28 July 2014 **Accepted** 13 September 2014

Introduction

With the introduction of fully integrated PET/CT cameras more than a decade ago, a new area in nuclear medicine was opened, combining the anatomic information of a diagnostic CT (D-CT) with physiology. As a result, the use of fluorine-18 fluorodeoxyglucose (^{18}F-FDG) PET/CT in tumour staging and therapy response assessment has increased markedly [1–3]. Inspired by the success of PET/CT, major efforts have been made to develop integrated PET/MR systems as MR has certain advantages over CT, providing higher soft tissue contrast and additional functional imaging capabilities. It has already been established that the information of a SPECT/CT is superior in diagnostic accuracy and confidence to that of SPECT and CT separately, especially in skeletal lesions [4–7]. The success of integrated imaging has thereby led to an increasing use of SPECT/CT and may lead to widespread clinical applications of PET/MR.

However, from a workflow and cost perspective, it is not obvious that fully integrated systems are the optimal solution for cost-effective image acquisition. A calculation of the scanning costs as a function of investment and operating costs showed that PET/CT is a cost-effective implementation of an integrated device while most current SPECT/CT systems are not because lengthy data acquisition on the SPECT system blocks fast data acquisition on the CT system during a large fraction of the imaging time [8]. Integration of two devices deployed in two neighbouring rooms by a patient transfer device (shuttle) could help to make SPECT/CT and potentially PET/MR systems more cost effective [8]. Integration of images from two separate devices with software-based image fusion is possible and has been used mainly for brain tumours [9], prostate [10] or pelvic tumours [11]; however, in body applications, any positional change of the patient will impair fusion accuracy and therefore only software-based fusion for PET and CT was not considered as an alternative for PET/CT [12].

We have developed a shuttle system to integrate PET, SPECT, D-CT and MR systems enabling the transfer of patients from one to the other scanning table without patient repositioning between scans. This allows 'hardware'-based image fusion. For the integration of MR with PET/CT, the shuttle system was designed such that MR surface coils could be installed and removed without

0143-3636 © 2014 Wolters Kluwer Health | Lippincott Williams & Wilkins DOI: 10.1097/MNM.0000000000000229

Table 1 PET/CT + MR patient characteristics

Number of patients (*n*)	31
Age (mean ± SD) (years)	56.3 ± 14.2
Male [*n* (%)]	19 (61)
Injected dose of ^{18}F-FDG (MBq)	348 ± 8.4
Region of MR scan	
Abdomen	15
Abdomen and pelvis	9
Chest	5
Chest and abdomen	1
Chest, abdomen and pelvis	1
Indications	
Head and neck [*n* (%)]	3 (9.6)
Oropharyngeal cancer	3
Thorax [*n* (%)]	11 (35.5)
Pleural mesothelioma	2
Bronchial carcinoma	4
Breast cancer	3
Oesophageal cancer	2
Lymphoma [*n* (%)]	5 (16.1)
Hodgkin lymphoma	3
Non-Hodgkin lymphoma	2
Abdominal [*n* (%)]	8 (25.8)
Cholangiocellular carcinoma	1
Pancreatic cancer	1
Colon cancer	6
Melanoma [*n* (%)]	4 (12.9)

^{18}F-FDG, fluorine-18 fluorodeoxyglucose.

moving the patient. Thus, surface coil-induced CT streak artefacts and PET attenuation artefacts could be avoided. We have already shown that lesion discrimination and anatomical mapping with this shuttle system is feasible with a fast two-point Dixon-based T1w 3D MRI sequence and leads to similar results when comparing lesion characterization and conspicuity with low-dose CT [13]. Furthermore, our group investigated the possibility of the use of MRI sequences for attenuation correction in a trimodality PET/CT + MR system [14]. Other groups are also investigating the feasibility and benefit of fully integrated versus in-line PET/MR systems [15]; however, a tool that allows the flexible combination of a several different imaging systems has not been developed or investigated as yet.

Therefore, the purpose of this study was to assess the registration accuracy of image fusion in two different settings: a trimodality PET/CT + MR system as well as a SPECT + D-CT system.

Materials and methods

Patients

In this institutional review board-approved prospective study, 43 patients underwent either sequential PET/CT + MR ($n = 31$) or SPECT + D-CT ($n = 12$) between July 2010 and June 2011 as a part of their clinical work-up. Patient characteristics are summarized in Table 1 for PET/CT + MR and Table 2 for SPECT + D-CT. All SPECT scans were performed for the assessment of osseous pathology.

Image acquisition

PET/CT + MR scanning

PET/CT imaging was performed on a full-ring, time-of-flight PET/CT system (Discovery PET/CT 690; GE Healthcare, Waukesha, Wisconsin, USA). Patients fasted for at least 4 h. Sixty minutes after an injection of 348 ± 8.4 MBq of ^{18}F-FDG low-dose CT and PET data were acquired. CT parameters were as follows: 50–79 mAs/slice, 120 kVp, a pitch of 0.984 : 1, collimation of 64 × 0.625 mm, field of view (FOV) of 50 cm, a noise index of 20%, reconstructed to images of 0.625 mm transverse pixel size and 3.75-mm slice thickness.

Table 2 SPECT + D-CT patient characteristics

Number of patients (*n*)	12
Age (mean ± SD) (years)	69.5 ± 6.9
Male [*n* (%)]	3 (25)
Injected dose of ^{99m}Tc-DPD (MBq)	669 ± 12
Field of view	
Knee	3
Lumbar spine	6
Pelvis	1
Lower leg	2
Indication	
Osseous metastasis [*n* (%)]	7 (58)
Breast cancer	6
Prostate cancer	1
Inflammatory disease [*n* (%)]	5 (42)
Prosthesis	3
Osteomyelitis	2

D-CT, diagnostic CT.

After PET/CT scanning, the patients were transferred to a 3-T MR system (Discovery MR750; GE Healthcare) installed in an adjacent room. In every patient, the MR protocol included an axial T1-weighted fast dual gradient echo MR sequence with fat-water reconstruction (TR 3.8 ms, TE_1 1.15 ms, TE_2 2.3 ms, FOV 48 cm, acquisition matrix 320 × 256, with a slice thickness 6.8 mm). The water images obtained were then used for the registration performance analysis.

PET/CT and MR gantry laser systems were used to position the patient board and automatically match the coordinate systems of both scanners to allow subsequent registration of the acquired data sets.

SPECT + CT scanning

SPECT data were acquired on a Hawkeye (Millennium VG; GE Healthcare) SPECT/CT system with integrated attenuation correction CT (Ac-CT) with a 128 × 128 matrix, a 30 s acquisition time per step and a 3° rotation step size. For emission data acquisition, low-energy/high-resolution collimators were used with an energy window of 140 ± 10% keV and a FOV of 40 cm. Ac-CT parameters were as follows: 2.5 mA, 140 kV, slice thickness 10 mm and matrix 256 × 256.

After SPECT imaging, the patient was transported to a 64-slice CT (Lightspeed VCT; GE Healthcare) for a D-CT of the region of interest. D-CT parameters were as follows: 70–300 mAs/slice, 120 kV, pitch 1.188, rotation time of 0.75 s, collimation of 64 × 0.625 mm, FOV of 50 cm, a noise index of 25%, reconstructed to images of

0.625-mm transverse pixel size and 1.5-mm slice thickness.

Cobalt-57 markers (CoM) were placed on the patients' shuttle board for manual matching of the coordinate systems of Hawkeye SPECT/CT and D-CT scanners and registration of the acquired data sets.

Patient transport/shuttle

The primary goal of this study was to assess the accuracy of image fusion with a flexible shuttle system that enables the sequentially integrated use of PET/CT and MR as well as SPECT and D-CT scanners. A flexible side-loading shuttle prototype was developed and constructed in collaboration with a prototyping engineering company (Innovation Design Center, Thalwil, Switzerland) (Fig. 1). Development and production costs for this prototype were around €22k.

For SPECT + CT, the patient transport board consisted of carbon fibre, whereas for the PET/CT + MR system, the transport board was built with fibre glass to minimize radio frequency attenuation effects. The MR scanner table was undocked and the patient was positioned on it outside the MR room as the current shuttle prototype is not built with MR-compatible materials. Patient transfer time was around 10 min for both settings. No special, additional restraints were used to reduce patient motion.

Assessment of image registration accuracy

PET/CT + MR system

For trimodality PET/CT + MR imaging fusion, the matched coordinate system allowed fully automatic image fusion of the CT and MR data sets without any software-based or manual registration correction. The misalignment from the automatic registration was recorded as offsets in the *X*-axis (lateral), *Y*-axis (anterior–-posterior) and *Z*-axis (cranio-caudal) between anatomical landmarks on CT and MRI. The magnitude of absolute displacement vector was calculated on the basis of the mean three-dimensional offsets. Anatomical landmarks least affected by respiratory motions and well depicted on both CT and MR images were selected: spine, pelvic bones and large paraspinal or pelvic muscles. In each patient, at least six anatomical landmarks were selected manually: three in the bony structures and three in the large muscles. Assessment of misalignment from the automatic registration was performed by two board-certified radiologists in consensus. Dedicated registration software package (Integrated Registration, Advantage Workstation 4.5; GE Healthcare) was used for the analysis.

SPECT + D-CT system

For SPECT + D-CT fusion, fully automatic coregistration with matched coordinate systems was not possible as

Fig. 1

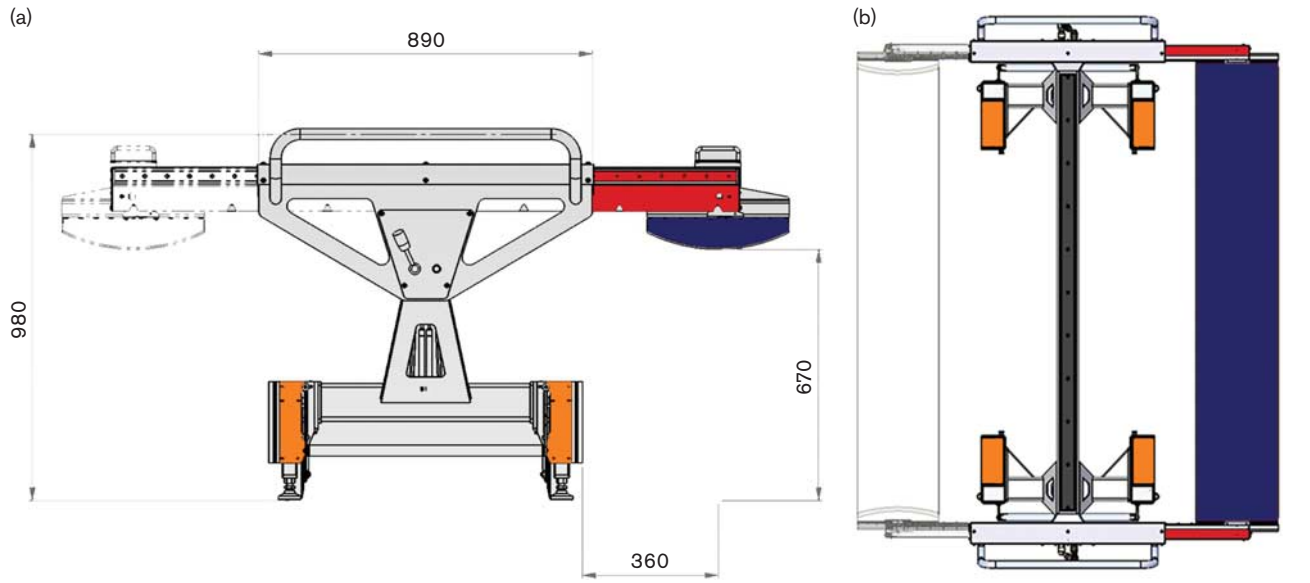

Side-loading shuttle. Frontal view (a) and top view (b) of the side-loading shuttle system, consisting of a metal trolley with counter balance weights (60 kg) on each side (orange). Two sliding 'arms' (red) hold a carbon or glass fibre board (blue) serving as a 'shuttle patient table', which can be slid either to the right or to the left of the shuttle system. This permits approaching and loading the patient onto a scanner table from either side. After sliding the board over the scanner table, the table is elevated until the board is entirely supported by it. Thereby, the board can be released from the arms, which are pulled back.

Fig. 2

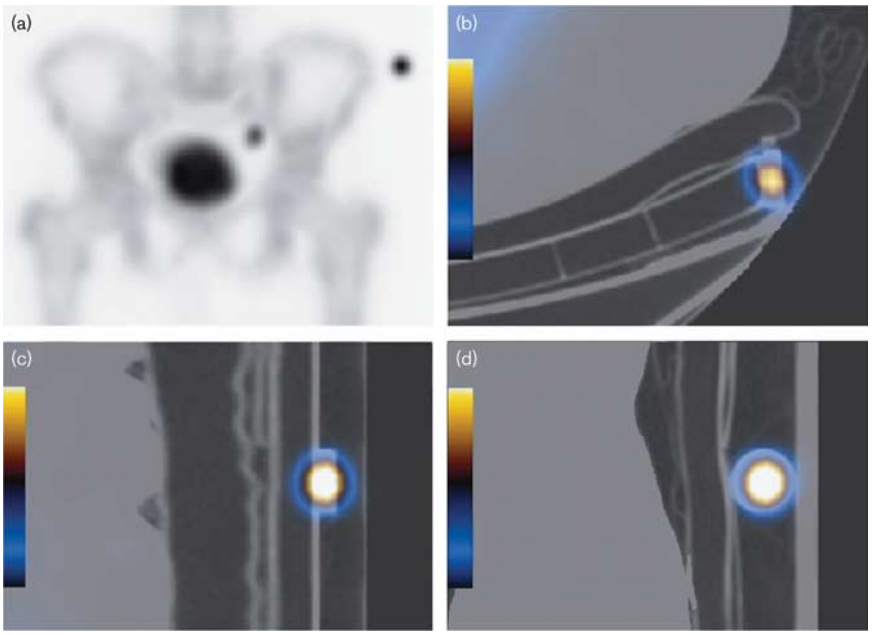

Cobalt registration marker. (a) SPECT MIP of the pelvis with a cobalt-57 marker (CoM) at the left lateral side of the carbon board. (b–d) Visual confirmation of accurate marker fusion in the fused SPECT + diagnostic CT (D-CT) images in (b) axial, (c) coronal and (d) sagittal views using the CoM.

Fig. 3

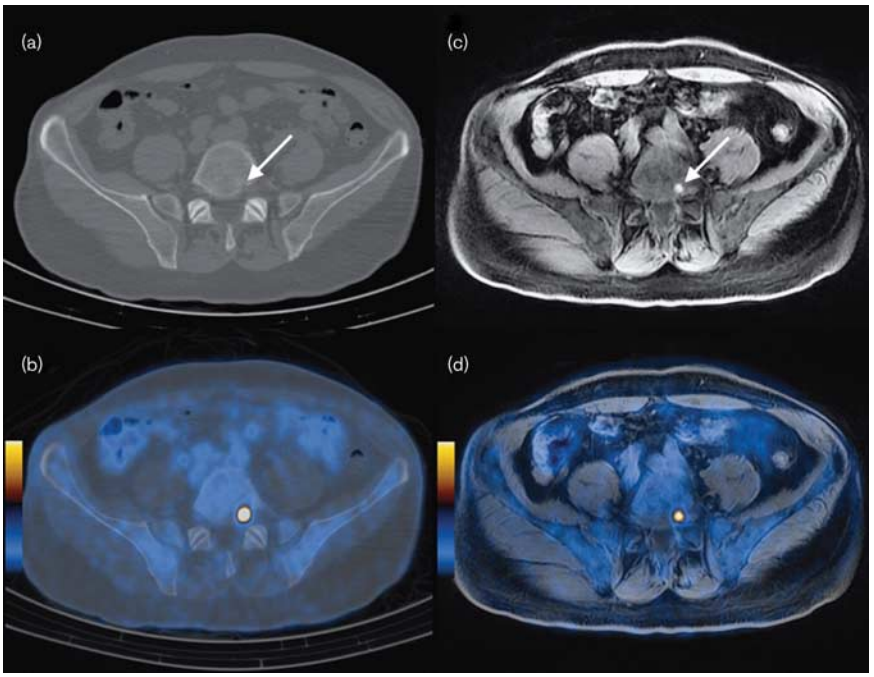

PET/CT + MR in a patient with melanoma. Bone metastasis in a 63-year-old man with malignant melanoma. (a) On CT cortical destruction is seen in the left posterior aspect of the L5 vertebral body (white arrow). (b) Fused fluorine-18 fluorodeoxyglucose (^{18}F-FDG) PET/CT image shows increased ^{18}F-FDG uptake in the osseous lesion. (c) Nonenhanced T1-weighted MR image acquired on a standalone MR scanner clearly shows the hyperintense lesion consistent with melanoma metastasis (white arrow). (d) Accurate PET/MR fusion of sequential PET and MR imaging achieved with the side-loading shuttle system with subsequent manual correction.

there is no laser patient positioning system for the Hawkeye SPECT/CT system. We therefore used external CoM attached to the shuttle table to align the coordinate systems and match SPECT and CT data (Fig. 2) with manual registration (Integrated Registration, Advantage Workstation 4.5; GE Healthcare). The accuracy of CoM-assisted image fusion was then verified against the Ac-CT by matching the bony structures between D-CT and Ac-CT datasets. Three anatomical landmarks were selected for each patient. The offsets between the landmarks were recorded in the *X*-axis (lateral), *Y*-axis (anterior–posterior) and *Z*-axis (craniocaudal). For each patient, the mean offset for the three landmarks was then calculated. The magnitude of the absolute displacement vector was calculated on the basis of the mean three-dimensional offsets.

Results

PET/CT + MR

The mean offset between CT and MR images for the PET/CT + MR setting was 8.1 ± 5.7 mm in the *X*-axis, 5.0 ± 4.0 mm in the *Y*-axis and 4.9 ± 5.6 mm in the *Z*-axis. The magnitude of the absolute displacement vector calculated on the basis of the mean three-dimensional offsets was 10.7 mm. Two clinical examples of sequential PET/CT + MR imaging with resulting accurate fusion of PET/MR images are presented in Figs 3 and 4.

SPECT + D-CT

The mean offset between anatomical landmarks on Ac-CT and D-CT in the SPECT + D-CT setting was 0.7 ± 0.8 mm in the *X*-axis, 2.1 ± 1.7 mm in the *Y*-axis and 0.8 ± 1.8 mm in the *Z*-axis. The magnitude of the absolute displacement vector calculated on the basis of the mean three-dimensional offsets was 2.4 mm. A clinical example of sequentially fused SPECT + D-CT images is shown in Fig. 5.

Discussion

The present results show that the principle of a flexible side-loading patient shuttle can be used to achieve 'hardware' fusion with offsets between PET/CT + MR of mean 10.7

Fig. 4

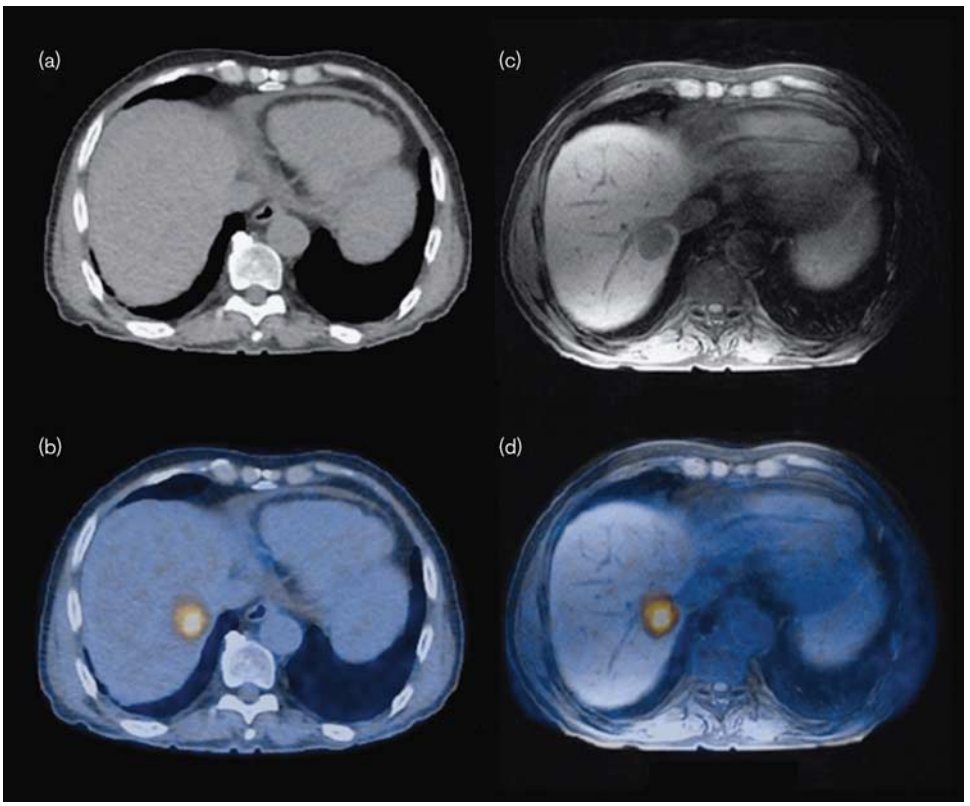

PET/CT + MR in a patient with colorectal cancer. Male patient (65 years old) with a liver metastasis of colorectal cancer in liver segment VII. (a) On nonenhanced CT image, no lesion is visible in the liver parenchyma. (b) Fused PET/CT images shows focal increased fluorine-18 fluorodeoxyglucose (^{18}F-FDG) uptake in liver segment VII. (c) Nonenhanced T1-weighted MR image acquired on a standalone MR scanner clearly shows a hypointense lesion in segment VII. (d) Accurate PET/MR fusion of sequential PET and MR imaging achieved with the shuttle system with subsequent manual correction, showing the hepatic metastasis in segment VII.

Fig. 5

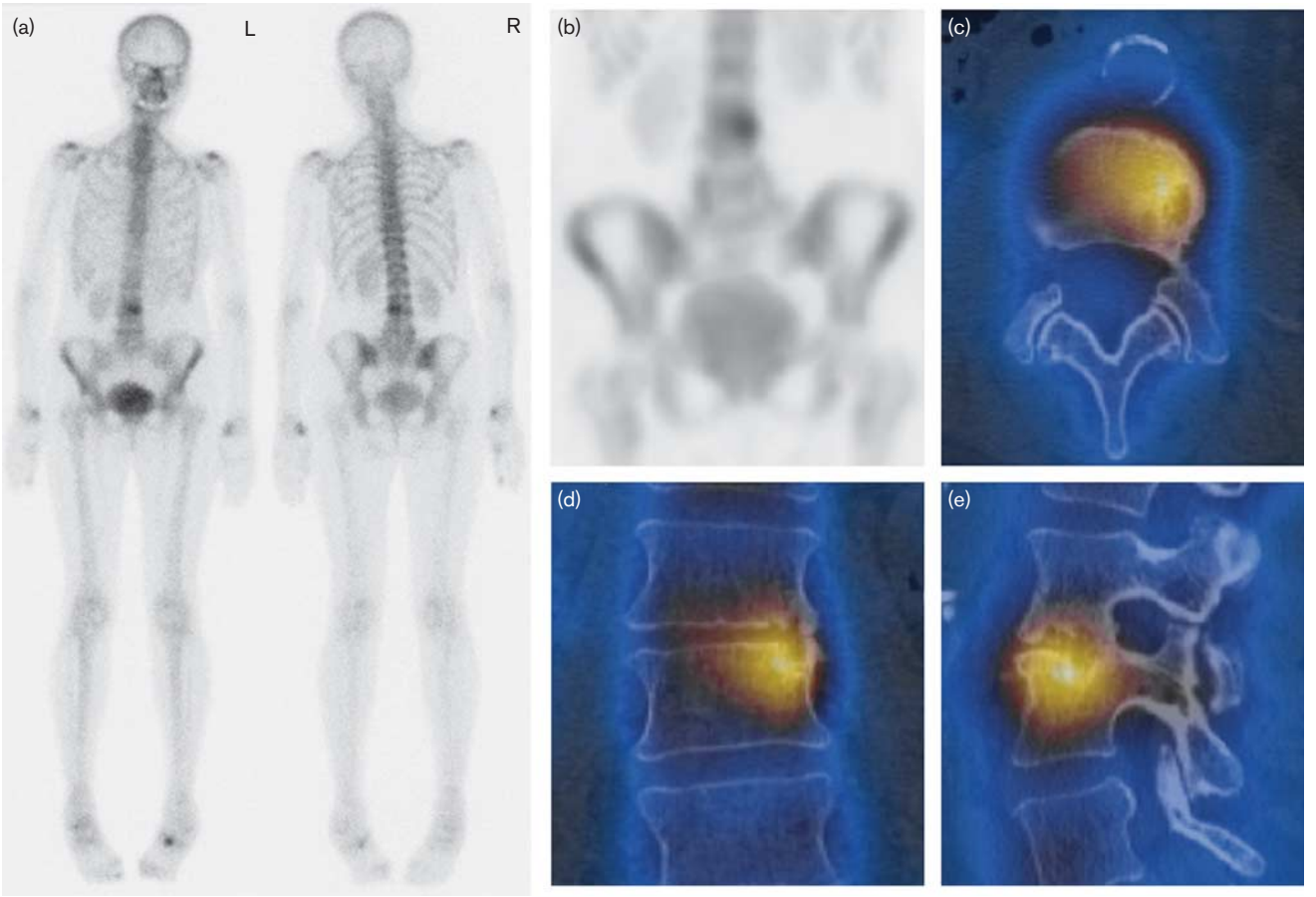

SPECT + diagnostic CT (D-CT) in a patient with breast cancer. A woman with breast cancer (71 years old), referred for staging. (a) Unclear lesion in the lumbar spine on whole-body ^{99m}Tc-DPD-scintigraphy. (b) SPECT MIP image showing the unclear lesion. (c–e) Fused SPECT + D-CT images in axial, coronal and sagittal view, respectively. Accurate fusion of sequentially acquired SPECT and D-CT images with the side-loading shuttle system allowed identification of the lesion as degenerative spondylosis L3/L4.

and 2.4 mm using fiducial markers with the SPECT + D-CT systems. Until now, only software-based image fusion data have been published for separate scanner systems such as SPECT + D-CT or PET/CT + MR [9–11,16–20]. Although the rigid structure of the skull ascertains that software fusion of brain structures is adequate, postural changes in the trunk and extremities may impair fusion accuracy [12].

Therefore, we developed and evaluated a dedicated shuttle system. In sequential integration of PET/CT and MR, the gantry laser systems can be used successfully to match the coordinate systems of both scanners. In the case of SPECT and D-CT integration, the approach utilizing cobalt sources attached to the shuttle system was developed and used to match the coordinate systems. For the trimodality PET/CT + MR system, the 'hardware' fusion of PET/CT and MR data provided registration between datasets with small offsets, showing the feasibility of this sequential approach with a dedicated patient shuttle system.

Although fully integrated SPECT with high-end CT scanner systems (≥16 slices) are available, less busy services may opt to install shuttle systems between their nuclear cameras and a nearby D-CT to be more cost effective [8]. The same could in fact be true for PET/MR implementations. Although fully integrated PET/MR have the advantage of simultaneous data acquisition without moving the patient or the table when imaging single FOVs, separate PET and MR systems have the advantage of full flexibility when placed in two separate rooms and might therefore be used more effectively. Furthermore, integrated 'hybrid' PET/MR or SPECT/CT systems are costly and beyond reach from the financial perspective for the majority of centres. A simple patient shuttle system could allow the integration of existing scanners to answer specific clinical questions without the need for costly investments.

The present study focused on image fusion accuracy arising from patient motion as well as transportation and

repositioning errors. It could be seen as a limitation that no phantom study is included to evaluate pure physical error arising from transportation and repositioning with the shuttle. However, as we were mainly interested in the performance in a daily clinical setting, patient data were analysed to evaluate the total robustness of the system. It should be taken into account that respiratory motion can cause considerable registration errors between the PET, CT and MR data. Therefore, in this study, anatomical structures least affected by respiratory motion were used for the analysis of misalignment.

A fully automatic coregistration of SPECT + D-CT data was not possible. However, manual fusion of the shuttle system cobalt sources (CoM) between SPECT and D-CT in a first step is tantamount for the laser positioning system. With this preparatory step, osseous landmarks in Ac-CT versus D-CT were only 1.2 ± 2.6 mm apart. Although not used in our study, potentially, metal and oil-containing markers attached to the shuttle table can be developed to match the coordination systems of PET/CT and MR in a similar way as for the SPECT D-CT system to complement the scanner gantry laser systems.

Further technical improvements of patient shuttle systems, such as interlocks of the shuttle with the imaging tables, might result in even more accurate coregistration between different modalities, minimizing operator dependence and obviating manual fusion.

Conclusion

Sequential PET/CT + MR and SPECT + D-CT imaging using a newly developed in-house solution for a dedicated patient shuttle system is feasible, resulting in mean offsets between data sets of 10.7 mm using the gantry laser system and 2.4 mm with fiducial markers.

Acknowledgements

This work was partially supported by a research grant from GE Healthcare, Waukesha, Wisconsin, USA.

Irene A. Burger was supported financially by Professor Dr Max Cloëtta Foundation (Switzerland) and the Swiss Society of Nuclear Medicine.

Andrei Samarin was supported by the European Union through the European Regional Development Fund.

Conflicts of interest

Fredrik Brandsberg is co-owner of Innovation Design Center, Thalwil, Switzerland. For the remaining authors there are no conflicts of interest.

References

1 Cohade C, Osman M, Leal J, Wahl RL. Direct comparison of (18)F-FDG PET and PET/CT in patients with colorectal carcinoma. *J Nucl Med* 2003; **44**:1797–1803.
2 Lardinois D, Weder W, Hany TF, Kamel EM, Korom S, Seifert B, *et al.* Staging of non-small-cell lung cancer with integrated positron-emission tomography and computed tomography. *N Engl J Med* 2003; **348**:2500–2507.
3 Von Schulthess GK, Steinert HC, Hany TF. Integrated PET/CT: current applications and future directions. *Radiology* 2006; **238**:405–422.
4 Delbeke D, Schöder H, Martin WH, Wahl RL. Hybrid imaging (SPECT/CT and PET/CT): improving therapeutic decisions. *Semin Nucl Med* 2009; **39**:308–340.
5 Even-Sapir E, Flusser G, Lerman H, Lievshitz G, Metser U. SPECT/multislice low-dose CT: a clinically relevant constituent in the imaging algorithm of nononcologic patients referred for bone scintigraphy. *J Nucl Med* 2007; **48**:319–324.
6 Helyar V, Mohan HK, Barwick T, Livieratos L, Gnanasegaran G, Clarke SE, Fogelman I. The added value of multislice SPECT/CT in patients with equivocal bony metastasis from carcinoma of the prostate. *Eur J Nucl Med Mol Imaging* 2010; **37**:706–713.
7 Papathanassiou D, Bruna-Muraille C, Jouannaud C, Gagneux-Lemoussu L, Eschard JP, Liehn JC. Single-photon emission computed tomography combined with computed tomography (SPECT/CT) in bone diseases. *Joint Bone Spine* 2009; **76**:474–480.
8 Von Schulthess GK, Burger C. Integrating imaging modalities: what makes sense from a workflow perspective? *Eur J Nucl Med Mol Imaging* 2010; **37**:980–990.
9 Grosu AL, Weber WA, Franz M, Stärk S, Piert M, Thamm R, *et al.* Reirradiation of recurrent high-grade gliomas using amino acid PET (SPECT)/CT/MRI image fusion to determine gross tumor volume for stereotactic fractionated radiotherapy. *Int J Radiat Oncol Biol Phys* 2005; **63**:511–519.
10 Park H, Wood D, Hussain H, Meyer CR, Shah RB, Johnson TD, *et al.* Introducing parametric fusion PET/MRI of primary prostate cancer. *J Nucl Med* 2012; **53**:546–551.
11 Vargas HA, Burger IA, Donati OF, Andikyan V, Lakhman Y, Goldman DA, *et al.* Magnetic resonance imaging/positron emission tomography provides a roadmap for surgical planning and serves as a predictive biomarker in patients with recurrent gynecological cancers undergoing pelvic exenteration. *Int J Gynecol Cancer* 2013; **23**:1512–1519.
12 Kim JH, Czernin J, Allen-Auerbach MS, Halpern BS, Fueger BJ, Hecht JR, *et al.* Comparison between ^{18}F-FDG PET, in-line PET/CT, and software fusion for restaging of recurrent colorectal cancer. *J Nucl Med* 2005; **46**:587–595.
13 Kuhn FP, Crook DW, Mader CE, Appenzeller P, von Schulthess GK, Schmid DT. Discrimination and anatomical mapping of PET-positive lesions: comparison of CT attenuation-corrected PET images with coregistered MR and CT images in the abdomen. *Eur J Nucl Med Mol Imaging* 2013; **40**:44–51.
14 Samarin A, Burger C, Wollenweber SD, Crook DW, Burger IA, Schmid DT, *et al.* PET/MR imaging of bone lesions – implications for PET quantification from imperfect attenuation correction. *Eur J Nucl Med Mol Imaging* 2012; **39**:1154–1160.
15 Cho ZH, Son YD, Choi EJ, Kim HK, Kim JH, Lee SY, *et al.* In-vivo human brain molecular imaging with a brain-dedicated PET/MRI system. *MAGMA* 2013; **26**:71–79.
16 Chowdhury FU, Scarsbrook AF. The role of hybrid SPECT-CT in oncology: current and emerging clinical applications. *Clin Radiol* 2008; **63**:241–251.
17 Donati OF, Hany TF, Reiner CS, von Schulthess GK, Marincek B, Seifert B, Weishaupt D. Value of retrospective fusion of PET and MR images in detection of hepatic metastases: comparison with ^{18}F-FDG PET/CT and Gd-EOB-DTPA-enhanced MRI. *J Nucl Med* 2010; **51**:692–696.
18 Kim SK, Choi HJ, Park SY, Lee HY, Seo SS, Yoo CW, *et al.* Additional value of MR/PET fusion compared with PET/CT in the detection of lymph node metastases in cervical cancer patients. *Eur J Cancer* 2009; **45**:2103–2109.
19 Nakamoto Y, Tamai K, Saga T, Higashi T, Hara T, Suga T, *et al.* Clinical value of image fusion from MR and PET in patients with head and neck cancer. *Mol Imaging Biol* 2009; **11**:46–53.
20 Patel CN, Chowdhury FU, Scarsbrook AF. Hybrid SPECT/CT: the end of 'unclear' medicine. *Postgrad Med J* 2009; **85**:606–613.